Journal of Sound and Vibration (2000) **237**(5), 775–791
doi:10.1006/jsvi.2000.3097, available online at http://www.idealibrary.com on IDEAL®

USE OF CROSS-TIME–FREQUENCY ESTIMATORS FOR STRUCTURAL IDENTIFICATION IN NON-STATIONARY CONDITIONS AND UNDER UNKNOWN EXCITATION

P. BONATO

NMRC, Boston University, 19 *Deerfield Street, Boston MA* 02215, *U.S.A.*

R. CERAVOLO AND A. DE STEFANO

Department of Structural and Geotechnical Engineering, Politecnico di Torino, c. Duca degli Abruzzi 24, 10129 *Torino, Italy. E-mail: ceravolo@athena.polito.it*

AND

F. MOLINARI

Department of Electronics, Politecnico di Torino, c. Duca degli Abruzzi 24, 10129 *Torino, Italy*

(*Received* 4 *January* 1999, *and in final form* 13 *March* 2000)

This paper introduces a new structural identification method for use in non-stationary conditions, which applies to structures and systems in normal serviceability conditions, under unknown excitation. The proposed method uses auto- and cross-time–frequency transforms of accelerometer signals recorded from the structure to identify the vibration modes. The transforms considered are those in Cohen's class which, in addition to possessing valuable properties for the analysis of mechanical signals, lend themselves to a clear interpretation in energy terms. This method enables modal parameters to be reliably estimated and an earlier technique proposed by the authors which was based on modal filters to be improved. It is further shown that the cross-correlation-based estimators are more effective than techniques based on auto-transformations, due to their noise-filtering properties. Finally, a method to refine the estimate of modal shapes, which avoids autocorrelation, is proposed. The accuracy of the procedure was assessed by means of numerical simulations.

1. INTRODUCTION

The monitoring of systems in normal service conditions is of paramount importance in a variety of fields where fault or damage detection is an issue. In some sectors, including civil structures, the use of techniques that exploit environmental excitation may avoid problems such as obstruction of road bridges or breaks in production processes. The use of environmental input gives rise to the need for analyzing non-stationary response signals, generally from accelerometers, which constitute the typical output of the systems monitored. When bi-linear transforms from Cohen's class are used, the system response is perceived in the time–frequency plane as the evolution of spectral components corresponding to the energy of the individual vibration modes [1–3]. The aim of this work is to show that auto- and cross-time–frequency based techniques can be used effectively in system identification in non-stationary conditions, under unknown excitation, and can replace traditional techniques. In other words, the proposed method does not require strict conditions about stationarity, but its performance is tied to modal component separability in the time–frequency plane. The technique is based on the assumption that the input of the system spans the frequency range of the vibration modes. The broader the spectrum of the input, the more accurate the identification.

A procedure proposed previously [4–7] involved the use of filters in the time domain to separate the modal components, and special frequency alignment algorithms for the determination of phase differences between signals. In fact, it is necessary for the determination of the modal shape relating to each individual vibration mode to estimate the amplitude as well as the phase relationship between signals.

With the method proposed here, the estimation of amplitude and phase information is based directly on the analysis of the auto- and cross-time–frequency transforms of the signals. This simplifies the procedure and does away with a critical step of the previous approach, i.e., the design of band-pass filters and their application in the time domain. In particular, amplitude ratios are determined directly from the ratio between the instantaneous amplitudes of the time–frequency representations of the signals. Phase relationships are estimated based on the phase of the cross-time-frequency representation of pairs of channels [8, 9].

Since the estimators provided by this new method are derived directly from two-dimensional functions of the time and frequency variables, they retain their dependence on time variables. Therefore they make it possible to determine the time evolution of the modal shape associated with a given frequency component and hence to establish *a posteriori*, i.e., at the end of the process, whether a given frequency value may or may not be a structural vibration mode. In linear time-invariant systems, modal signals are characterized by the fact that amplitude and phase relationships are constant and therefore the modal shape to which they give rise is characterized by stability over time.

Numerical examples are presented in section 6 of the paper, showing how the proposed procedure was used to identify a three-degrees-of-freedom (d.o.f.s) model (of a shear-type frame).

2. COHEN CLASS AUTO- AND CROSS-TRANSFORMS

Time–frequency transforms are spectral analysis tools designed to study the harmonic content of signals as a function of time [1]. All the transforms belonging to the Cohen class can be written in the form:

$$D_x(t,f) = \iiint x\left(t' + \frac{\tau}{2}\right) x^*\left(t' - \frac{\tau}{2}\right) g(\theta,\tau)\, \mathrm{e}^{-\mathrm{j}2\pi\theta(t'-t)}\, \mathrm{e}^{-\mathrm{j}2\pi f\tau}\, \mathrm{d}\theta\, \mathrm{d}t'\, \mathrm{d}\tau, \qquad (1)$$

where $D_x(t,f)$ is the time–frequency distribution, $x(t)$ is the input signal, $x^*(t)$ is its complex conjugate, t is the time, f is the frequency, τ is the time lag, θ is the frequency lag, and $g(\theta, \tau)$ is the kernel of the transform. From equation (1) it can be seen that the time-frequency transform is computed by applying a kernel to the instantaneous autocorrelation function, which is defined as

$$acf_x(t,\tau) = x\left(t + \frac{\tau}{2}\right) x^*\left(t - \frac{\tau}{2}\right). \qquad (2)$$

TABLE 1

Properties of the time–frequency distributions belonging to the Cohen class and associated conditions on the kernel of the transform

	Property	Conditions on the Kernel
P1	Time and frequency shift	$g(\theta, \tau)$ independent of t and f
P2	Time marginal	$g(\theta, 0) = 1 \forall\theta$
P3	Frequency marginal	$g(0, \tau) = 1\ \forall\tau$
P4	Instantaneous frequency	$\left.\frac{\partial g(\theta, \tau)}{\partial \tau}\right\rvert_{\tau=0} = 0\ \forall\theta$
P5	Group delay	$\left.\frac{\partial g(\theta, \tau)}{\partial \theta}\right\rvert_{\theta=0} = 0\ \forall\tau$
P6	Attenuation of interfering terms	$g(\theta, \tau)$ attenuates terms apart from the axes in the ambiguity domain

The generalized instantaneous autocorrelation function (i.e., equation (2) after the kernel application) is Fourier-transformed, thus obtaining the time-frequency representation of the input signal. The kernel characteristics are strictly associated with distribution properties, and hence it is possible to ensure that the transform will possess a number of specific properties by selecting kernels that hold certain characteristics. Table 1 summarizes some properties that are particularly relevant to the identification of structures [1].

Cohen's class groups together all bi-linear transforms that are invariant to time and frequency shifts (P1). This property is relevant to the technique proposed in this paper since it makes it possible to locate correctly, in the time–frequency domain, a harmonic component present in the signal. If this property does not hold, modal waveforms at different frequencies which occur at different points in time will be represented differently thus leading to possible errors in the modal identification procedure.

Another essential property is the so-called marginal property (P2 and P3). By choosing a kernel which is unitary over the axes of the ambiguity domain (i.e. the domain defined by time and frequency lags), it is possible to ensure that the representation obtained in the time–frequency plane will retain the energy properties of the signal. Specifically, by integrating the distribution along the time axis, the spectral density of energy is obtained. Through integration along the frequency axis the instantaneous energy is obtained. These properties are relevant to the identification of structures since both the amplitudes of the modal vibrations and their frequencies are computed to derive the modal shapes. If the time–frequency distribution does not satisfy the marginals, it is expected that the estimated modal frequencies and amplitudes may be affected by a significant estimation error.

Properties P4 and P5 (i.e., instantaneous frequency and group delay) are desirable properties for the identification of the modal frequencies and for the estimation of the phase relationships among the signals recorded from the structure investigated.

Finally, because of the bi-linearity of the time–frequency transformation the distribution of multi-component signals is affected by spurious terms [1] often indicated as interference terms. These terms are due to the cross-products among the signal components and they are usually located away from the origin of the ambiguity plane. Their presence in the time–frequency domain may make the interpretation of the distribution difficult and compromise the reliability of the technique proposed here. However, the kernel of the transform can attenuate them significantly if it is properly designed. For the application that is investigated in this paper, the kernel needs to be chosen so that it attenuates terms away from the axes of the ambiguity domain (P6).

Among all the transforms belonging to the Cohen class, the simplest one is the Wigner–Ville transform. This transform is characterized by a unitary kernel over the entire (θ, τ) plane. It can be demonstrated that it has all the properties listed in Table 1, with the exception of P6. In the last decade, a variety of kernels was proposed to attenuate the interference terms without significantly affecting the auto-terms of the representation [1]. Choi and Williams [10] first proposed a transform using an exponential kernel in (θ, τ) that has all the properties listed in Table 1. This transform makes it possible to screen out efficiently some of the interfering terms originated by the quadratic nature of the autocorrelation product, thus facilitating the interpretation of the time–frequency distribution. Although an appropriate choice of the kernel is fundamental to obtain reliable results from the identification process, it is worth noting that the method herein proposed does not rely on a specific kernel. A discussion of the way the kernel choice affects the identification of the modal shapes is provided in the section of the paper that presents the application of the method to synthesized data (see section 6).

For each Cohen class transform, it is possible to define a cross-time–frequency representation by replacing the instantaneous autocorrelation function of an individual signal by the instantaneous cross-correlation function, defined as

$$xcf_{x,y}(t, \tau) = x\left(t + \frac{\tau}{2}\right)y^*\left(t - \frac{\tau}{2}\right), \tag{3}$$

where x and y indicate two input signals. Cross-representations differ from auto-time–frequency distributions. For instance, time–frequency representations of the Cohen class are real (i.e., the imaginary part is null). In fact, the instantaneous autocorrelation function, as reported in equation (2), is Hermitian and thus its Fourier transform is real. This is not the case when cross-transformations are considered, since the instantaneous cross-correlation function is not necessarily Hermitian. On the other hand, the relationship between the real and imaginary part of a cross-time–frequency representation is related to the phase between corresponding components of the two signals, x and y. In addition, when x and y contain common components (i.e., the same vibration modes) they are located in the ambiguity domain as the terms of an auto-transformation, whereas components that are not simultaneously present on both the signals are located in the ambiguity domain as interference terms. This observation implies that components that are present simultaneously on both the channels are "transformed" as components of an auto-time–frequency representation and thus the properties of Table 1 apply. Also, components that are not simultaneously present on both the signals are filtered as interference terms and thus P6 in Table 1 applies. Further details are provided in the following sections.

3. TIME-FREQUENCY ESTIMATORS FOR MODAL IDENTIFICATION

It is assumed that signals acquired on a structure that can be modelled in a discrete manner with n d.o.f.s. Let $s_i(t)$ be the displacement at the ith position, $q^{(k)}(t)$ the displacement associated with the kth vibration mode, and finally, let $u_i^{(k)}$ be a term of the matrix of normalized eigenvectors, which decouples the motion equations; then

$$s_i(t) = \sum_k u_i^{(k)} q^{(k)}(t). \tag{4}$$

The sum in equation (4) is extended to the vibration modes as detected at the ith position. If the structure, subjected to excitation, is instrumented with simultaneous acquisition channels according to some of the n d.o.f.s, then the individual modal component of the ith channel, which appears in the form of an energy peak in the time–frequency domain, can be written in its complex form as

$$s_i^{(k)}(t) = u_i^{(k)} q^{(k)}(t) = u_i^{(k)} \tilde{q}^{(k)}(t)\, \mathrm{e}^{\mathrm{j}2\pi f^{(k)} t}, \tag{5}$$

where $\tilde{q}^{(k)}(t) = A^{(k)}(t)\, \mathrm{e}^{\mathrm{j}\varphi^{(k)}(t)}$ is a baseband signal, having introduced the following quantities, related to the kth mode: $A^{(k)}(t)$ and $\varphi^{(k)}(t)$, amplitude- and phase-modulating waveforms; $f^{(k)}$, natural frequency; $u_i^{(k)}$, amplitude of the modal shape at the ith position. If the spectrum of $q^{(k)}(t)$ is single-sided, the complex form in equation (5) also represents the analytic signal.

The instantaneous autocorrelation function of a modal component $s_i^{(k)}(t)$ is

$$\begin{aligned} acf_{s_i^{(k)}}(t,\tau) &= u_i^{(k)^2} \tilde{q}^{(k)}\left(t + \frac{\tau}{2}\right) \mathrm{e}^{\mathrm{j}2\pi f^{(k)}(t+\tau/2)}\, \tilde{q}^{(k)*}\left(t - \frac{\tau}{2}\right) \mathrm{e}^{-\mathrm{j}2\pi f^{(k)}(t-\tau/2)} \\ &= u_i^{(k)^2} acf_{\tilde{q}^{(k)}}(t,\tau)\, \mathrm{e}^{\mathrm{j}2\pi f^{(k)}\tau}, \end{aligned} \tag{6}$$

where $acf_{\tilde{q}^{(k)}}(t,\tau)$ indicates the instantaneous autocorrelation function of the amplitude modulating waveform associated with the kth vibration mode as recorded from the ith channel. By Fourier transforming the instantaneous autocorrelation function, the Wigner–Ville transform of $s_i^{(k)}(t)$ is

$$WV_{s_i^{(k)}}(t,f) = u_i^{(k)^2} F_{\tau\to f}\{acf_{\tilde{q}^{(k)}}(t,\tau)\, \mathrm{e}^{\mathrm{j}2\pi f^{(k)}\tau}\} = u_i^{(k)^2}\, WV_{\tilde{q}^{(k)}}(t,f) *_f \delta(f - f^{(k)}), \tag{7}$$

where $F_{\tau\to f}\{\ \}$ indicates the Fourier transform from τ (time-lag) to f (frequency), $WV_{\tilde{q}^{(k)}}(t,f)$ is the Wigner–Ville transform of the modulating waveform, $*_f$ is the convolution in frequency, and $\delta(\ )$ is the unit impulse.

From equation (7) it is apparent that the transform's energy is concentrated around the modal frequency and the shape of the distribution is determined by the time–frequency transform of the modulating waveform $\tilde{q}^{(k)}(t)$. Since the shape of the modulating waveform is maintained in the time–frequency domain, the amplitude ratio between two modal components (except for the sign) can be determined directly from the time–frequency representations in the following manner:

$$\begin{aligned} AR(t) &= \sqrt{\frac{WV_{s_i^{(k)}}(t,f)}{WV_{s_j^{(k)}}(t,f)}}\Bigg|_{f=f^{(k)}} \\ &= \sqrt{\frac{u_i^{(k)^2}\, WV_{\tilde{q}^{(k)}}(t,f) *_f \delta(f-f^{(k)})}{u_j^{(k)^2}\, WV_{\tilde{q}^{(k)}}(t,f) *_f \delta(f-f^{(k)})}}\Bigg|_{f=f^{(k)}} = \frac{u_i^{(k)}}{u_j^{(k)}}. \end{aligned} \tag{8}$$

$AR(t)$ is the time–frequency estimator for the amplitude ratio between two modal components. In the time–frequency domain, the possibility of detecting changes in the frequency content of the signal makes it possible to interpret correctly the physical implications of the signal characteristics even in the case of non-stationary excitations, for instance by distinguishing the components that are constantly present in the signal.

When using a different Cohen class transform, other than the Wigner–Ville transform, the following expression is obtained:

$$D_x(t,f) = \Gamma(t,f) *_{t,f} WV_x(t,f), \tag{9}$$

where $D_x(t,f)$ indicates a Cohen class representation, $\Gamma(t,f)$ is the kernel of the transform in the time–frequency domain, and $*_{t,f}$ is the double convolution in time and frequency. Therefore, the time–frequency estimator defined by equation (8) leads to the ratio between the amplitude of the modal shape at the ith and jth positions for any Cohen class representation. In multi-component signals, when interference and auto-terms are superimposed, the use of a kernel capable of attenuating the interference terms leads to an increase of the reliability of the amplitude ratio estimation.

Phase differences can also be estimated in the time–frequency domain thus leading to a time-dependent output. The phase difference between two channels, for a given decoupled mode, must remain constant (0 or π for real modes). Auto-time–frequency representations do not contain information on the phase, but this information may be derived using cross-time–frequency representations.

Consider, for instance, the following two modal signals, picked up at positions i and j, whose phase difference $\Delta\varphi_{ij}^{(k)}$ is assumed to be constant in time:

$$s_i^{(k)}(t) = u_i^{(k)}\,\tilde{q}^{(k)}(t)\,\mathrm{e}^{\mathrm{j}2\pi f^{(k)}t}$$

$$s_j^{(k)}(t) = u_j^{(k)}\,\tilde{q}^{(k)}(t)\,\mathrm{e}^{\mathrm{j}2\pi f^{(k)}t + \mathrm{j}\Delta\varphi_{ij}^{(k)}}. \tag{10}$$

Their instantaneous cross-correlation function is

$$xcf_{s_i^{(k)}s_j^{(k)}}(t,\tau) = u_i^{(k)}\,\tilde{q}^{(k)}\left(t+\frac{\tau}{2}\right)\mathrm{e}^{\mathrm{j}2\pi f^{(k)}(t+\tau/2)}\,u_j^{(k)}\,\tilde{q}^{(k)*}\left(t-\frac{\tau}{2}\right)\mathrm{e}^{\mathrm{j}2\pi f^{(k)}(t-\tau/2)}\,\mathrm{e}^{-\mathrm{j}\Delta\varphi_{ij}^{(k)}}$$

$$= u_i^{(k)}u_j^{(k)}\,acf_{\tilde{q}^{(k)}}(t,\tau)\,\mathrm{e}^{\mathrm{j}2\pi f^{(k)}\tau}\,\mathrm{e}^{-\mathrm{j}\Delta\varphi_{ij}^{(k)}} \tag{11}$$

and hence the cross-Wigner–Ville representation (XWV) can be written as:

$$XWV_{s_i^{(k)}s_j^{(k)}}(t,f) = u_i^{(k)}u_j^{(k)}\,\mathrm{e}^{-\mathrm{j}\Delta\varphi_{ij}^{(k)}}F_{\tau\to f}\{acf_{\tilde{q}^{(k)}}(t,\tau)\,\mathrm{e}^{\mathrm{j}2\pi f^{(k)}\tau}\}$$

$$= u_i^{(k)}u_j^{(k)}\,WV_{\tilde{q}^{(k)}}(t,f-f^{(k)})\,\mathrm{e}^{-\mathrm{j}\Delta\varphi_{ij}^{(k)}}. \tag{12}$$

This equation shows that it is possible to define the estimator for the phase difference between two modal components as

$$PH(t) = phase\{XWV_{s_i^{(k)}s_j^{(k)}}(t,f)\}|_{f=f^{(k)}} = \Delta\varphi_{ij}^{(k)}. \tag{13}$$

As for the amplitude ratio estimator defined by equation (8), it can be shown that the general expression in equation (13) is valid for any real distribution belonging to the Cohen class.

4. MODAL PARAMETER IDENTIFICATION

The estimators defined in the previous section retain the dependence on time, and hence make it possible to establish *a posteriori*, i.e., at the end of the process, whether a given frequency value may or may not be a vibration mode of the structure. In fact, when one analyses linear time-invariant systems, decoupled modal signals are characterized by amplitude and phase relationships that are not time-dependent and therefore their modal shape is constant over time.

The identification of modal frequencies therefore reduces to a search for the particular values $f = f^{(k)}$ for which the estimators remain constant with respect to the time variable, in general by resorting to multiple criteria techniques [11, 12]. Having identified the frequencies, the estimators supply directly the temporal evolution of the amplitude and phase ratios, i.e., the modal shapes.

Multi-component signals are now considered. In this case, the bi-dimensional estimators assume the following form, valid for any transforms $D(t,f)$ of the Cohen class:

$$AR(t,f) = \sqrt{\frac{D_{s_i}(t,f)}{D_{s_j}(t,f)}} = \sqrt{\frac{\Gamma(t,f) *_{t,f} WV_{s_i}(t,f)}{\Gamma(t,f) *_{t,f} WV_{s_j}(t,f)}}, \quad (14a)$$

$$PH(t,f) = phase\{D_{s_i,s_j}(t,f)\} = phase\{\Gamma(t,f) *_{t,f} XWV_{s_i,s_j}(t,f)\}. \quad (14b)$$

In the general case of cross-correlations between channels, a bi-linear distribution will consist of auto- and cross-terms; therefore the cross-time–frequency distribution

$$D_{s_is_j}(t,f) = \int_{-\infty}^{+\infty}\int_{-\infty}^{+\infty}\int_{-\infty}^{+\infty} s_i(t'+\tau/2)s_j^*(t'-\tau/2)g(\theta,\tau)\,e^{-j2\pi\theta(t'-t)}\,e^{-j2\pi f\tau}\,d\theta\,dt'\,d\tau \quad (15)$$

may be expanded as follows

$$D_{s_is_j}(t,f) = \sum_k\sum_h u_i^{(k)}u_j^{(h)}D_{q^{(k)}q^{(h)}}(t,f)$$

$$= \sum_k u_i^{(k)}u_j^{(k)}D_{q^{(k)}}(t,f) + \sum_{k\neq h} u_i^{(k)}u_j^{(h)}D_{q^{(k)}q^{(h)}}(t,f). \quad (16)$$

The cross-terms may be filtered using an appropriate kernel. This operation can be viewed clearly by referring to the ambiguity function domain, which is dual with respect to the time–frequency domain [1]. In this domain, the cross-terms are displaced from the axes as the interference terms in an auto-transformation, as discussed in the following subsection.

4.1. INTERFERENCE TERM FILTERING

The time–frequency distribution formulated in equation (15) has a dual image in the ambiguity function domain [1, 2]. In fact, for two components $q^{(k)}(t)$ and $q^{(h)}(t)$,

$$M_{q^{(k)}q^{(h)}}(\theta,\tau) = g(\theta,\tau)AF_{q^{(k)}q^{(h)}}(\theta,\tau), \quad (17)$$

where

$$AF_{q^{(k)}q^{(h)}}(\theta,\tau) = \int_{-\infty}^{\infty} q^{(k)}(t+\tau/2)\,q^{(h)*}(t-\tau/2)\,e^{-j2\pi\theta t}\,dt, \quad (18)$$

where $M_{q^{(k)}q^{(h)}}(\theta,\tau)$ is the characteristic function and $AF_{q^{(k)}q^{(h)}}(\theta,\tau)$ the ambiguity ($k = h$) or cross-ambiguity ($k \neq h$) function.

For two displacement signals the characteristic function can be written as follows:

$$M_{s_is_j}(t,f) = \sum_k u_i^{(k)}u_j^{(k)}M_{q^{(k)}q^{(k)}}(\theta,\tau) + \sum_{k\neq h}\sum u_i^{(k)}u_j^{(h)}M_{q^{(k)}q^{(h)}}(\theta,\tau). \quad (19)$$

The corresponding instantaneous cross-correlation function is:

$$R_{q^{(k)}q^{(h)}}(t, \tau) = A^{(k)}(t + \tau/2)\, A^{(h)*}(t - \tau/2)\, \mathrm{e}^{\mathrm{j}2\pi((f^{(k)} + f^{(h)})/2)\tau}\, \mathrm{e}^{\mathrm{j}2\pi(f^{(k)} - f^{(h)})t}$$
$$\mathrm{e}^{\mathrm{j}(\phi^{(k)}(t + \tau/2) - \phi^{(h)}(t - \tau/2))}. \quad (20)$$

From equation (20) it can be seen that, in the ambiguity function domain, the modal components ($f^{(k)} = f^{(h)}$) fall on the τ-axis ($\theta = 0$), while the cross-components ($f^{(k)} \neq f^{(h)}$) fall at a distance $f^{(k)} - f^{(h)}$ from the τ-axis. This makes apparent why the use of a kernel that rejects the terms displaced from the time-lag axis leads to the selection of the components common to both channels [10].

4.2. MODAL FREQUENCY LOCALIZATION

It should be observed that, once the cross-terms have been filtered, a potential source of error in the identification of the vibration modes is a possible close coupling among different components. The components in the frequency domain are uncoupled as long as the phase and frequency modulation is negligible, thus the ratio between the time–frequency representations, as estimated at the modal frequencies, will approximate to the square of the modal amplitude ratio. In the time–frequency domain, a single component is uncoupled when it produces a separate component in the time–frequency plane, which develops around its instantaneous frequency. In comparison with classical frequency analysis, time–frequency cross-transforms between channels are able to filter products among different components that, although closely coupled in frequency, are uncorrelated in time (e.g., flexural and torsional modes of bridges) [4].

It can be concluded that the reliability of the proposed estimator and the identifiability of the structure investigated are related to single-component separability in the time-frequency plane, i.e., both to close coupling of modal frequency and to excitation type. The capability of the cross-time–frequency transform of separating the signal components is improved by using kernels that are highly selective in the ambiguity function domain. Using highly selective kernels, therefore, allows the amplitude ratio and phase difference estimators to be approximated for each modal frequency even for multi-component signals:

$$AR(t,f)|_{f=f^{(k)}} = \sqrt{\frac{D_{s_i}(t,f)}{D_{s_j}(t,f)}}\Bigg|_{f=f^{(k)}} \cong \sqrt{\frac{\sum_k u_i^{(k)^2} D_{\tilde{q}^{(k)}}(t,f-f^{(k)})}{\sum_k u_i^{(k)^2} D_{\tilde{q}^{(k)}}(t,f-f^{(k)})}} = \frac{u_i^{(k)}}{u_j^{(k)}}, \quad (21a)$$

$$PH(t,f)|_{f=f^{(k)}} = phase\{D_{s_i,s_j}(t,f)\}|_{f=f^{(k)}}$$
$$\cong phase\left\{\sum_k u_i^{(k)} u_j^{(k)} D_{\tilde{q}^{(k)}}(t,f-f^{(k)})\right\}\Bigg|_{f=f^{(k)}} = \Delta\varphi_{ij}^{(k)}. \quad (21b)$$

In frequency intervals where a single-modal component is predominant, the estimators tend to lead to a constant value in time. As this property is progressively more closely satisfied up to an actual constant value at the modal frequencies, the latter can be identified by searching the minima of the following functions:

$$\int_0^T [AR(t,f) - \overline{AR}]^2\, \mathrm{d}t, \quad (22a)$$

$$\int_0^T [PH(t,f) - \overline{PH}]^2\, \mathrm{d}t, \quad (22b)$$

where T is the length of the analyzed signal and $\overline{AR}$ and $\overline{PH}$ indicate the mean value of the amplitude ratio and phase difference respectively.

5. REFINEMENT OF THE ESTIMATION

Once the modal frequencies have been identified, a more accurate method may be used to refine the modal shape evaluation.

A synthetic signal $z^{(k)}(t)$ can be generated as a sinusoid (i.e., the corresponding analytic signal) with frequency equal to a specific modal frequency and with phase φ_z:

$$z^{(k)}(t) = K\mathrm{e}^{\mathrm{j}2\pi f^{(k)}t + \mathrm{j}\varphi_z}. \tag{23}$$

The cross-Wigner–Ville representation (XWV) of this synthetic signal and the data recorded at the ith position can be written as

$$XWV_{s_i z^{(k)}}(t,f) = \sum_h u_i^{(h)} XWV_{q^{(h)}z^{(k)}}(t,f) = u_i^{(k)} XWV_{q^{(k)}z^{(k)}}(t,f) + \sum_{h \neq k} u_i^{(h)} XWV_{q^{(h)}z^{(k)}}(t,f), \tag{24}$$

where

$$XWV_{q^{(k)}z^{(k)}}(t,f) = K\mathrm{e}^{-\mathrm{j}\varphi_z} F_{\tau\to f}\left\{\tilde{q}^{(k)}\left(t+\frac{\tau}{2}\right)\right\} *_\theta \delta(\theta - f^{(k)}),$$

$$XWV_{q^{(h)}z^{(k)}}(t,f) = K\mathrm{e}^{-\mathrm{j}\varphi_z}\mathrm{e}^{\mathrm{j}2\pi(f^{(h)}-f^{(k)})} F_{t\to f}\left\{\tilde{q}^{(h)}\left(t+\frac{\tau}{2}\right)\right\} *_\theta \delta\left(\theta - \frac{f^{(h)}+f^{(k)}}{2}\right). \tag{25}$$

The corresponding ambiguity functions are, respectively,

$$AF_{q^{(k)}z^{(k)}}(\theta,\tau) = F^{-1}_{t\to\theta}\{xcf_{q^{(k)}z^{(k)}}(t,\tau)\} = K\mathrm{e}^{-\mathrm{j}\varphi_z}\mathrm{e}^{\mathrm{j}2\pi f^{(k)}\tau} F^{-1}_{t\to\theta}\left\{\tilde{q}^{(k)}\left(t+\frac{\tau}{2}\right)\right\},$$

$$AF_{q^{(k)}z^{(k)}}(\theta,\tau) = F^{-1}_{t\to\theta}\{xcf_{q^{(k)}z^{(k)}}(t,\tau)\}$$

$$= K\mathrm{e}^{-\mathrm{j}\varphi_z}\mathrm{e}^{\mathrm{j}2\pi((f^{(h)}+f^{(k)})/2)\tau} F^{-1}_{t\to\theta}\left\{\tilde{q}^{(h)}\left(t+\frac{\tau}{2}\right)\right\} * \delta(\theta - (f^{(h)} - f^{(k)})). \tag{26}$$

The latter equations show that, in the ambiguity domain, the cross-terms ($k \neq h$) are located away from the θ-axis. The choice of selective kernels, which retain only the components near the θ-axis, makes it possible to attenuate the interference terms and emphasize the modal component that it is intended to identify.

When a distribution $D(t,f)$ is considered, whose kernel efficiently attenuates the interference terms and it is used to derive the cross-time–frequency representation of the synthesized signal and the accelerometer signal at the ith position, then:

$$D_{s_i z^{(k)}}(t,f) \cong K u_i^{(k)} D_{q^{(k)}z^{(k)}}(t,f). \tag{27}$$

When this procedure is repeated for the signals at the ith and jth position, the modal shape estimators can be taken as

$$AR(t,f)|_{f=f^{(k)}} = \left|\frac{D_{s_i z^{(k)}}(t,f)}{D_{s_j z^{(k)}}(t,f)}\right|\Bigg|_{f=f^{(k)}}, \tag{28a}$$

$$PH(t,f)|_{f=f^{(k)}} = phase\left\{\frac{D_{s_i z^{(k)}}(t,f)}{D_{s_j z^{(k)}}(t,f)}\right\}\Bigg|_{f=f^{(k)}}. \tag{28b}$$

This procedure is advantageous over that defined by equations (21), since the modal parameters are derived from the cross-time–frequency representation between a multi-component signal and a monocomponent one. Consequently, in equations (28) the number and location of cross-terms (i.e., interference terms) is less critical when compared with the cross-time–frequency representation of two multi-component signals. This observation is discussed in the following section, where an example is proposed that illustrates the advantages of the refinement method proposed in this section.

6. SAMPLE APPLICATION

In the following, a sample application of the procedure defined in the previous sections to data synthesized using a model of a three-storey shear-type frame is presented. Figure 1 summarizes the characteristics of the simulated structure. The outputs corresponding to different storeys of the simulated building (Figure 1, right side) were obtained for different input signals. Two excitations were used, namely a sine sweep from 0·1 to 3 Hz and a seismic excitation (an accelerometer measurement from the Loma Prieta earthquake 1989, Natural Science Building at UC Santa Cruz, E/W direction, peak ground acceleration = 0·4248g).

Single storey oscillator:
Data

Mass	40 tons
Frequency	1 Hz
Damping	2%

Modal parameters
of the model

Frequencies	0·445 Hz, 1·2470 Hz, 1·8019 Hz
Modal damping	0·89%, 2·49%, 3·6%
1-st eigenvector	{0·3184, 0·5970, 0·7363}
2-nd eigenvector	{0·7363, 0·3184, − 0·5970}
3-rd eigenvector	{0·5970, − 0·7363, 0·3184}

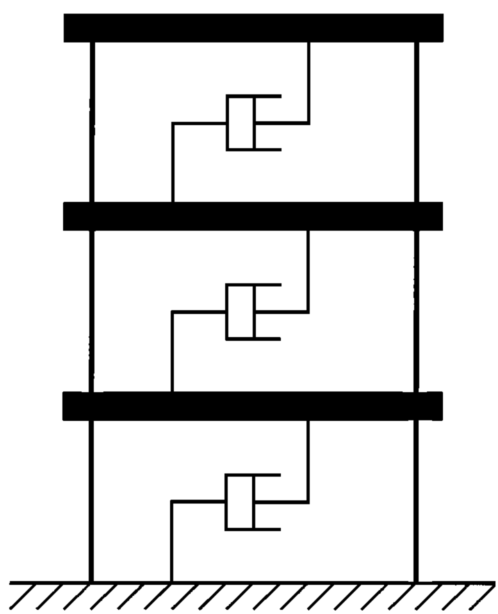

Figure 1. Case study. On the left side of the figure, the tables summarize the system's characteristics. On the right side, the plot shows schematically the simulated structure.

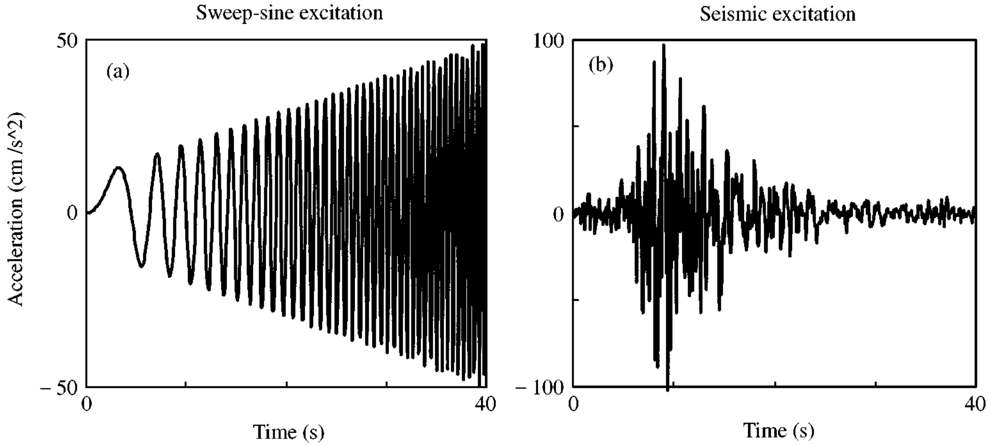

Figure 2. Inputs of the linear system, i.e., excitation applied at the support of the simulated structure. (a) Sine sweep ranging from 0·1 Hz to 3 Hz. (b) Data collected during the Loma Prieta earthquake 1989, Natural Science Building at UC Santa Cruz, E/W direction, PGA = 0·4248g.

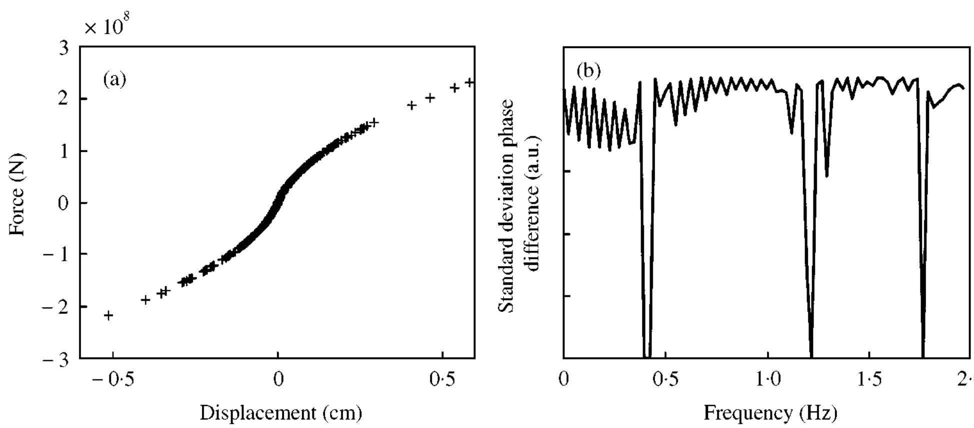

Figure 3. Simulated non-linearity and identification of the modal frequencies. Plot (a) shows the quadratic-softening type characteristic of the simulated structure. Plot (b) represents the standard deviation of the phase difference computed for the second storey of the simulated structure with respect to the first storey as a function of frequency. The minima identified the pseudo-modal frequencies.

Both the inputs are shown in Figure 2. Different inputs were used to investigate how the method performs under different types of non-stationarity of the input signal. It is worth noting that knowledge of the excitation is not necessary to identify the structure, since the method introduced in this paper utilizes only the response signals, namely the outputs recorded at different storeys.

In addition to the linear case, the application of this approach to the simulated structure when modified by introducing a quadratic-softening-type non-linearity according to the characteristic illustrated in Figure 3(a) was also investigated. In the latter case, the response of the non-linear system to the sine-sweep excitation was studied to assess the effect of "mild" non-linearities on the identification procedure. In all the simulated cases, the estimation was carried out according to equations (21) and (28) and the modal frequencies were computed by detecting the occurrence of minima in the standard deviation of the phase difference (equation (22b)). Although the proposed approach does not rely on a specific kernel belonging to the Cohen class of distributions, the reliability of the estimation procedure depends on the choice of the kernel of the transform. An optimal kernel for the identification procedure must be capable of efficiently attenuating the interference terms, since their attenuation implies a decrease of the error that affects the amplitude ratio and phase difference estimates. In the proposed sample application, the attenuation of the interference terms did not result to be a particularly critical point. Satisfactory results were obtained using a Choi–Williams transform [10] with $\sigma = 0{\cdot}5$. Possible criteria to choose the kernel of the transform are discussed in a following subsection.

6.1. MODAL FREQUENCY ESTIMATION

The cases examined are: (1) linear frame, sine sweep excitation at the support; (2) linear frame, seismic excitation at the support; and (3) frame with quadratic-softening-type non-linearity, sine-sweep excitation at the support. Table 2 summarizes the modal frequencies estimated for the three investigated cases and allows the comparison with the theoretical values.

The modal frequencies reported in Table 2 were estimated from the lowest three minima in the plots representing the standard deviation of the phase difference for different channels as illustrated in Figures 4(a) and 4(b) and Figure 3(b). These plots were all obtained using Choi–Williams distributions with $\sigma = 0{\cdot}5$ [10] to derive the amplitude ratios and phase differences according to equations (21).

Figure 3 refers to the case when a linear system with sine-sweep input (Figure 4(a) and seismic input (Figure 4(b)) respectively were simulated. In both cases, the estimated modal frequencies are extremely close to the theoretical ones. However, it is apparent that the variability of the plot in the case corresponding to a seismic input is significantly higher than that observed when a sine-sweep excitation was applied to the model. Such different behaviour is likely related to the different type of non-stationarity of the input in the two simulated cases.

Figure 3(b) shows that similar modal frequencies (i.e., pseudo-modal frequencies) are identified when analyzing the simulated non-linear structure. This suggests that the proposed method is capable of performing the identification of vibration components in presence of both a non-stationary input as well as "mild" non-linearities. Also, the variability of the curve obtained when the sine sweep was applied to the non-linear frame was higher than that observed when the same input was applied to the linear frame. This

TABLE 2

Theoretical and identified modal frequencies obtained by applying the proposed method under different inputs (sine sweep and earthquake) and constitutive laws (linear and non-linear)

Modal frequency	Constitutive law	Excitation	1st (Hz)	2nd (Hz)	3rd (Hz)
Theoretical	Linear		0·445	1·247	1·802
Identified	Linear	Sine sweep	0·45	1·25	1·80
Identified	Linear	Earthquake	0·45	1·25	1·78
Identified	Non-linear (Figure 3(a))	Sine sweep	0·42†	1·15†	1·76†

† Pseudo-modal frequency.

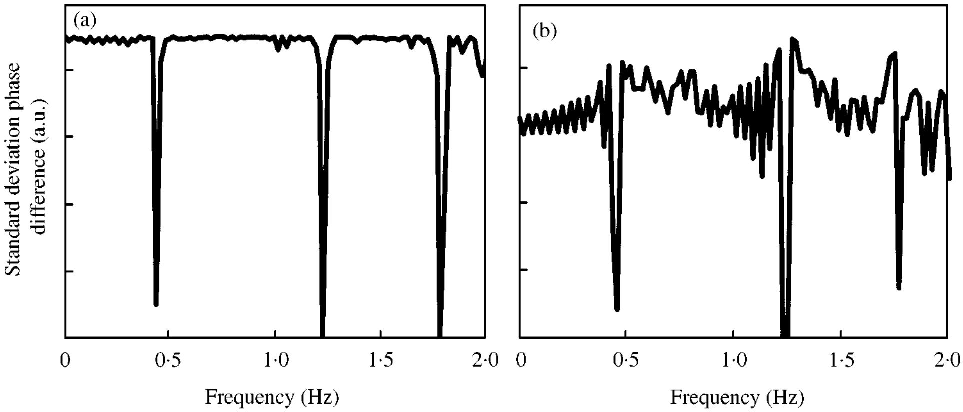

Figure 4. Standard deviation of the phase difference between the channel corresponding to the second storey of the simulated structure and the reference channel (first storey) as a function of frequency. Plot (a) corresponds to the case when a linear system was simulated and a sine-sweep excitation was used as input to the structure. Plot (b) is relative to the case of seismic excitation. The three minima (on both the plots) identify the modal frequencies.

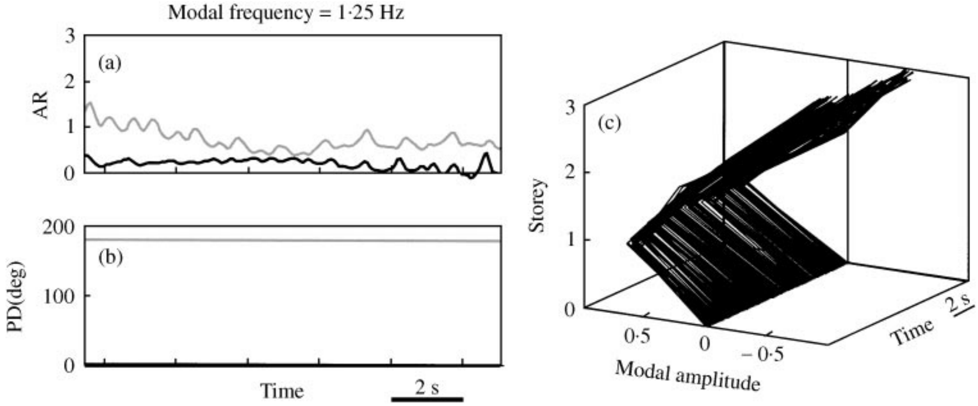

Figure 5. Evolution through time of modal amplitude ratios (a) and modal phase differences (b), as determined with respect to the reference channel (first storey) for the second and third storeys. Data are relative to the second mode. The light and dark lines indicate the amplitude ratio and phase difference computed for the second storey and third storey respectively. Plot (c) shows the time evolution of the modal shape as reconstructed using amplitude ratios and phase differences. Data were obtained when simulating a linear system with sine-sweep excitation and using the method summarized by equations (21).

suggests that “mild” non-linearities increase the variability of the parameter utilized to identify the modal frequencies as already observed for different type of non-stationarity of the input.

Once the modal frequencies are identified, amplitude ratios and phase differences can be used to derive the modal shapes associated with the different modal frequencies, i.e., their evolution in time can be estimated. The results for the second-modal shape are illustrated in Figure 5. Amplitude ratios and phase differences were computed taking the channel corresponding to the first storey as a reference. It is worth noting that the modal shape is expected to be constant in time unless in presence of non-linear behaviour, but this is not the case when one considers the amplitude ratios reported in Figure 5(a). In this plot, the spurious oscillations which affect the estimated modal parameters may be related to a non-optimal choice of the kernel of the transform, as will be discussed in the following section.

6.2. MODAL SHAPE IDENTIFICATION

Once the modal frequencies are identified, the method presented in section 5 to refine the estimation of the modal shapes may be used. For each identified modal frequency a sinusoidal waveform with frequency equal to the modal frequency is generated and equations (28) are used.

Figure 6 shows the amplitude ratios and phase differences for the second modal frequency derived by means of the procedure proposed in section 5. The reference channel is the accelerometer signal corresponding to the first storey. If a comparison is made between the estimates obtained by equations (21) (Figure 5) and the results derived using equations (28) (Figure 6), it is apparent that the modal shape estimated by the latter technique is considerably more reliable. The same technique was used for all the three identified modal frequencies. The estimated average modal shapes are represented in Figure 7 for all the three modal frequencies. The estimates are extremely close to the theoretical modal shapes shown in Table 3, where the reconstructed eigenvectors associated with the simulated structure are compared with the theoretical values.

6.3. CHOICE OF THE KERNEL

In the sample application presented in the previous section, the choice of the kernel of the time–frequency transform was not particularly critical. In actual applications to real data, the kernel choice may dramatically affect the estimation procedure. The capability of the kernel of the transform to attenuate the interference terms is expected to be an important factor when interference terms and autocomponents are superimposed. Problems may arise, for instance, in complex mechanical systems and, in general, when modal frequencies are spaced too closely. When the signal characteristics are totally unknown, adaptive methods

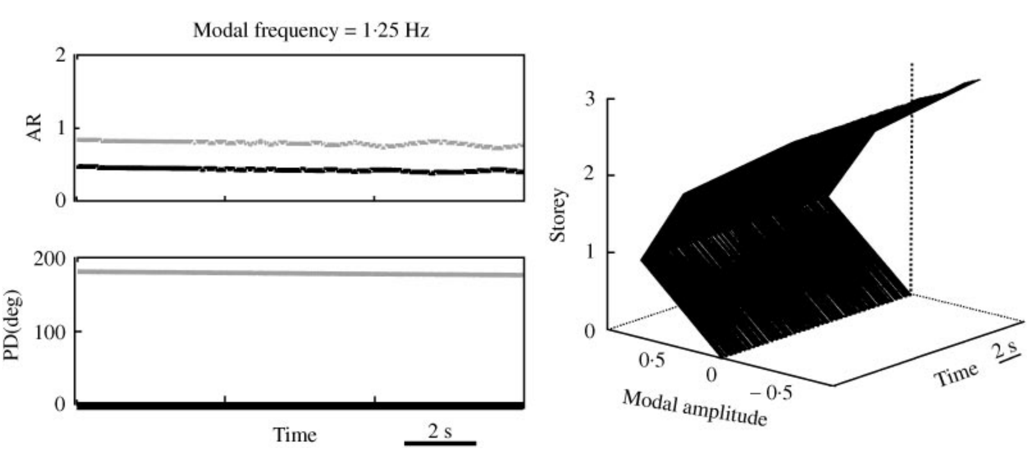

Figure 6. Modal amplitude ratios (a), modal phase differences (b), and timeevolution of the modal shape (c) as in Figure 3. In this case, however, the modal parameters are computed using the refinement method illustrated in Section 5 and summarized by equations (28).

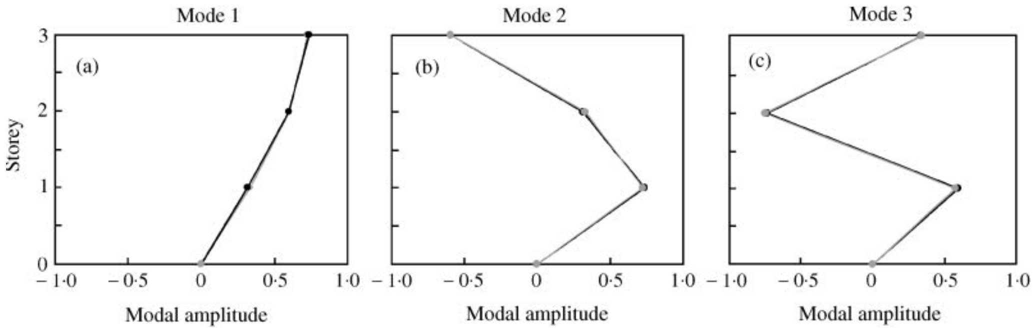

Figure. 7. Estimated modal shapes. The three lines, i.e., (a) continuous line, (b) dotted line, and (c) dashed line show the first, second, and third modal shape respectively.

TABLE 3

Theoretical and estimated eigenvectors for the three identified modal frequencies

Estimated modal frequency (Hz)	Theoretical eigenvector	Estimated eigenvector
0·45	[0·3184 0·5970 0·7363]	[0·3361 0·6032 0·7233]
1·25	[0·7363 0·3184 − 0·5970]	[0·7295 0·3320 − 0·5980]
1·80	[0·5970 − 0·7363 0·3184]	[0·5782 − 0·7500 0·3211]

[13–15] as well as design procedures based on the characteristics of the ambiguity function of the analyzed signal [16–19] could be useful. These approaches may offer a kernel geometry more suitable than the Choi–Williams kernel to reject components related to the cross-products among the vibration modes. In fact, such terms are parallel to the time-lag axis in the ambiguity domain and thus the Choi–Williams kernel might fail in attenuating them sufficiently. The referenced approaches may also provide a kernel with flatter passband and narrower transition regions in the ambiguity domain than the Choi–Williams. It must be emphasized, however, that when one uses the refinement approach proposed in section 5, possible drawbacks on the estimation of the modal shape related to the interference terms are dramatically reduced. In fact, the cross-correlation with a single-frequency component, as performed when a sinusoidal waveform is synthezised, implies that there will be no spurious terms centred on the frequency that corresponds to the analyzed modal component.

7. CONCLUSIONS

This paper proposes a new identification method, based on a number of estimators defined in the time–frequency domain. This technique applies to structures and systems in normal serviceability conditions, under unknown excitation.

Numerical tests led to satisfactory results, providing support for the theoretical considerations. The results show that it is possible to separate the modal frequencies from typical excitation components. The proposed method appears to offer a higher level of resolution compared to traditional techniques. Furthermore, the method was shown to be robust to the presence of markedly non-stationary excitation, e.g., seismic input, and to slightly non-linear conditions.

In this paper, it was further shown that the cross-correlation-based estimators are more effective than those based on the autocorrelation, mainly because of the intrinsic filtering of the noise components provided by cross-correlation-based methods. Based on this observation, it is proposed to refine the modal shape estimates using a procedure that solely relies on cross-time–frequency transforms.

Although the application to real structures is expected to be more challenging than the application to simulated data (due to measurement noise, non-linearity, non-classical damping etc.), the proposed method builds upon an earlier procedure [4] that was shown to be effective in applications to real structures (bridges and buildings). This earlier methodology made use of modal filters that could increase the estimation error affecting the reconstructed modal shapes. The estimators proposed here are more reliable since they avoid possible distortions of the signal related to the filtering procedure. The results suggest that this novel identification method leads to great effectiveness and facilitates the automation of the identification process. Further studies will be devoted to the definition of time–frequency estimators for structural damping identification.

ACKNOWLEDGMENTS

The authors would like to thank Dr Zeynep Erim and Dr Virgil Stokes for their comments on an early version of the manuscript. They also would like to thank the anonymous reviewers for their comments and suggestions.

REFERENCES

1. L. Cohen 1995 *Time–Frequency Analysis*. Englewood Cliffs, NJ: Prentice-Hall.
2. F. Hlawatsch and G. F. Boudreaux-Bartels 1992 *IEEE Signal Processing Magazine* **9**, 21–67. Linear and quadratic time–frequency signal representations.
3. J. K. Hammond and P. R. White 1996 *Journal of Sound and Vibration* **190**, 419–447. The analysis of non-stationary signals using time–frequency methods.
4. P. Bonato, R. Ceravolo and A. De Stefano 1997 *Journal of Engineering Mechanics* (*ASCE*) **123**, 1260–1267. Time–frequency and ambiguity function approaches in structural identification.
5. R. Brincker, A. De Stefano and B. Piombo 1996 *Proceedings of* 14*th International Modal Analysis Conference*, *Society of Experimental Mechanics*, *Bethel*, *CT*, *U.S.A.*, 477–482. Ambient data to analyse the dynamic behaviour of bridges: a first comparison between different techniques.
6. R. Ceravolo 1996 Ph.D. thesis, 10, Dept. Struct. Eng. Politecnico di Torino, Turin (in Italian). Metodi Dinamici Avanzati in Diagnostica Strutturale.
7. A. De Stefano, R. Ceravolo, P. Bonato, G. Gagliati and M. Knaflitz 1996 *Proceedings* 14*th International Modal Analysis Conference*, *Society of Experimental Mechanics*, *Bethel*, *CT*, *U.S.A.*, 470–476. Analysis of ambient vibration data from Queensborough Bridge using Cohen class time–frequency distributions.
8. P. Bonato, R. Ceravolo and A. De Stefano and F. Molinari 1998 *Damage Assessment of Structures* (M. D. Gilchrist, J. M. Dulieu-Barton and K. Worden, editors), 363–372. Uetikon-Zuerich, Switzerland: Trans Tech Publications. A new cross-time–frequency method for the structural identification of mechanical systems in nonstationary conditions.
9. P. Bonato, R. Ceravolo and A. De Stefano and F. Molinari 1998 *Proceedings of the IEEE International Symposium on Time–Frequency and Time-Scale Analysis*, *Pittsburgh*, *Pennsylvania*, *U.S.A.*, 445–448. Time–frequency and cross-time–frequency based techniques for the structural identification of systems.
10. H. I. Choi and W. J. Williams 1989 *IEEE Transactions on Acoustics*, *Speech and Signal Processing* **37**, 862–871. Improved time–frequency representation of multicomponent signals using exponential kernels.

11. C. A. BANA (editor) 1990 *Readings in Multiplecriteria Decision Aid*. Berlin, GE: Springer-Verlag.
12. G. FANDER and J. SPRONK (editors) 1985 *Multiplecriteria Decision Methods and Applications*. Berlin, GE: Springer-Verlag.
13. R. G. BARANIUK and D. L. JONES 1993 *IEEE Transactions on Acoustics, Speech and Signal Processing* **41**, 1589–1602. A signal-dependent time–frequency representation: optimal kernel design.
14. R. G. BARANIUK and D. L. JONES 1993 *Signal Processing* **32**, 263–284. A radially gaussian, signal-dependent time–frequency representation.
15. R. G. BARANIUK and D. L. JONES 1994 *IEEE Transactions on Acoustics, Speech and Signal Processing* **42**, 134–146. A signal-dependent time–frequency representation: fast algorithm for optimal kernel design.
16. F. AUGER 1994 *IEEE Signal Processing Letters* **1**, 9–11. Some simple parameter determination rules for the generalized Choi-Williams and Butterworth distributions.
17. A. H. COSTA and G. F. BOUDREAUX-BARTELS 1995 *IEEE Transactions on Acoustics Speech and Signal Processing* **43**, 2283–2301. Design of time–frequency representations using a multiform, tiltable exponential kernel.
18. A. PAPPANDREOU and G. F. BOUDREAUX-BARTELS 1993 *IEEE Transactions on Acoustics, Speech and Signal Processing* **41**, 463–472. Generalization of the Choi-Williams distribution and the Butterworth distribution for time–frequency analysis.
19. T. H. SANG and W. J. WILLIAMS 1995 *Proceedings IEEE Accoustic Signal Speech Process* **5**, 997–1000. Rényi information and signal-dependent optimal kernel design.